

We are IntechOpen, the world's leading publisher of Open Access books Built by scientists, for scientists

6,900

Open access books available

186,000

International authors and editors

200M

Downloads

Our authors are among the

154

Countries delivered to

TOP 1%

most cited scientists

12.2%

Contributors from top 500 universities



WEB OF SCIENCE™

Selection of our books indexed in the Book Citation Index
in Web of Science™ Core Collection (BKCI)

Interested in publishing with us?
Contact book.department@intechopen.com

Numbers displayed above are based on latest data collected.
For more information visit www.intechopen.com



Challenges in Rietveld Refinement and Structure Visualization in Ceramics

Touseef Ahmad Para and Shaibal Kanti Sarkar

Abstract

The most common and basic characterization in the field of material science is the almighty X-ray diffraction (XRD). In every institute, every research report and every manuscript, concerning material properties, the X-ray diffraction pattern is essentially found. Although the basis of these works relies on the fact that X-ray diffraction pattern was found to be matching with some structure in a database, the in depth significance of the various characteristic diffraction manifestations of various physical characters are rarely discussed. Most of the researchers (especially beginners) are either not aware of the prowess of X-ray based characterizations, or have not been introduced to it properly or may be sometimes they are not interested in its results at all. The decreased interest (later) in the results from such studies might be for not being productive enough for time spending or non-effectiveness in justifying the motivation of the work. The former two are more related to the availability and accessibility of study material for the development of core concepts. Most of the institutes always do not have access to the span-wide scientific literature and the researchers joining these institutions are partly affected. In this context the effective open-access and free availability of intech-open, it is prudent to at least attempt to accumulate, assimilated and aggregate the concepts related to X-ray diffraction in a single package. The chapter is an attempt in the path of this route.

Keywords: X-ray diffraction, space group, polyhedra, powder diffraction, Rietveld refinement, structure visualization

1. Introduction

Much has been written and learnt about powder diffraction in last two decades. The journey that began in 1910 with the Bragg father-son duo publishing their first paper on crystal structure determination using ionization spectrometer, a century later there are still perks and connives that have not been widely explored [1–3]. The meticulous solution to the single crystal NaCl structure by the Braggs was achieved by solving symmetry equations for thousands of positions within a unit cell of unknown symmetry, without the help of modern computational prowess [3–8]. As Mike Glazer put it in very powerful words, “It was the gifted mind of Lawrence Bragg seeing symmetries in space and numbers that enabled them to reach a solution much quickly than anticipated” [3, 5]. In addition, W L Bragg’s consideration of diffraction from crystals as merely reflections from crystal planes, simplified the theory around the structure determination considerably [9]. In just

few months, Braggs determined structure of NaCl, KCl, KBr, CaF₂, Cu₂O, ZnS, NaNO₃, some calcites and diamond from their respective single crystals [10].

The year 1914, Max von Laue was awarded Noble prize for his discovery of the diffraction of X-rays by crystals [11, 12] followed by 1915 prize for their services in the analysis of crystal structure by means of X-rays to W H and W L Bragg [6] itself concatenates the importance of crystal structure determination. In following years, Debye and Scherrer extended the theory from single crystal to powder diffraction, presenting the complete theory of powder diffraction patterns and crystal structures used today (*squared sums of hkl ordered triplets*) [13–16]. Although Scherrer, Debye and Hull solved structures of many materials, it was not until modern computational boom that new, more complex and low symmetry system could be solved via powder diffraction pattern [17–23]. In the quest of achieving a suitable pathway for attaining a solution of powder X-ray diffraction many niche-limited attempts like maximum likelihood method [24, 25], anomalous dispersion, maximum entropy method, line profile fitting [26] etc. were made abundantly in 1950s and 60s. Hugo Rietveld in 1960s came up with one such method, employing least square iteration principle to statistically estimate the weighted contribution of every point on a powder XRD pattern [27]. The method now known as Rietveld refinement was the first step towards full profile whole powder pattern fitting method for x-ray and neutron diffraction data.

2. Rietveld refinement

It was 1969, 27 copies of a 162 Kilobytes program were sent to different institutes all over the world. The program was accompaniment of paper published in Journal of Applied Crystallography titled “A Profile refinement Method for Nuclear and Magnetic Structures” by Hugo Rietveld. Within a span of a decade 200 structures were refined from powder diffraction data [26–28]. The method we all know as Rietveld refinement method, made possible to refine whole profile with parameters including half-width, zero shift, cell parameters [29], asymmetry correction [30, 31], preferred orientation correction [32, 33], overall scale factor, overall isotropic temperature factor, fractional coordinates of the atoms, atomic isotropic temperature, occupation numbers and the components of the magnetic vectors of each atom. The algorithm this program followed is summed up in **Figure 1**. In subsequent versions of the method, Rietveld introduced residual values (R values), allowing for a quantitative judgment of the refinement quality. Most of the findings and equations, which Rietveld published, are still used nowadays in their original form [14, 20, 21, 34–37].

In 1994, International Union of Crystallography (IUCr) constituted a commission on powder diffraction with the purpose of diving into the status of the world of scientific community in general and crystallographic community in particular and focus on the practical aspects of data collection, refinement software, data interpretations, future endeavors etc. [38]. The commission proposed certain protocols and few guidelines for data collection, background contribution, peak-shape function, refinement of profile parameters, Fourier analysis, refinement of structural parameters, geometric restraints, estimated standard deviation, interpretation of R values and some common problems with their possible solutions. Although the Hill and Cranswick [38–41] commission on powder diffraction formulated a set of general guidelines that encompassed the recommendations with some explanatory and cautionary notes regarding Rietveld refinement their application in the aspect for a newcomer are not totally encompassed [42, 43]. The reason is not the ineffectiveness, obsolescence or incomprehension but rather the scattered nature of

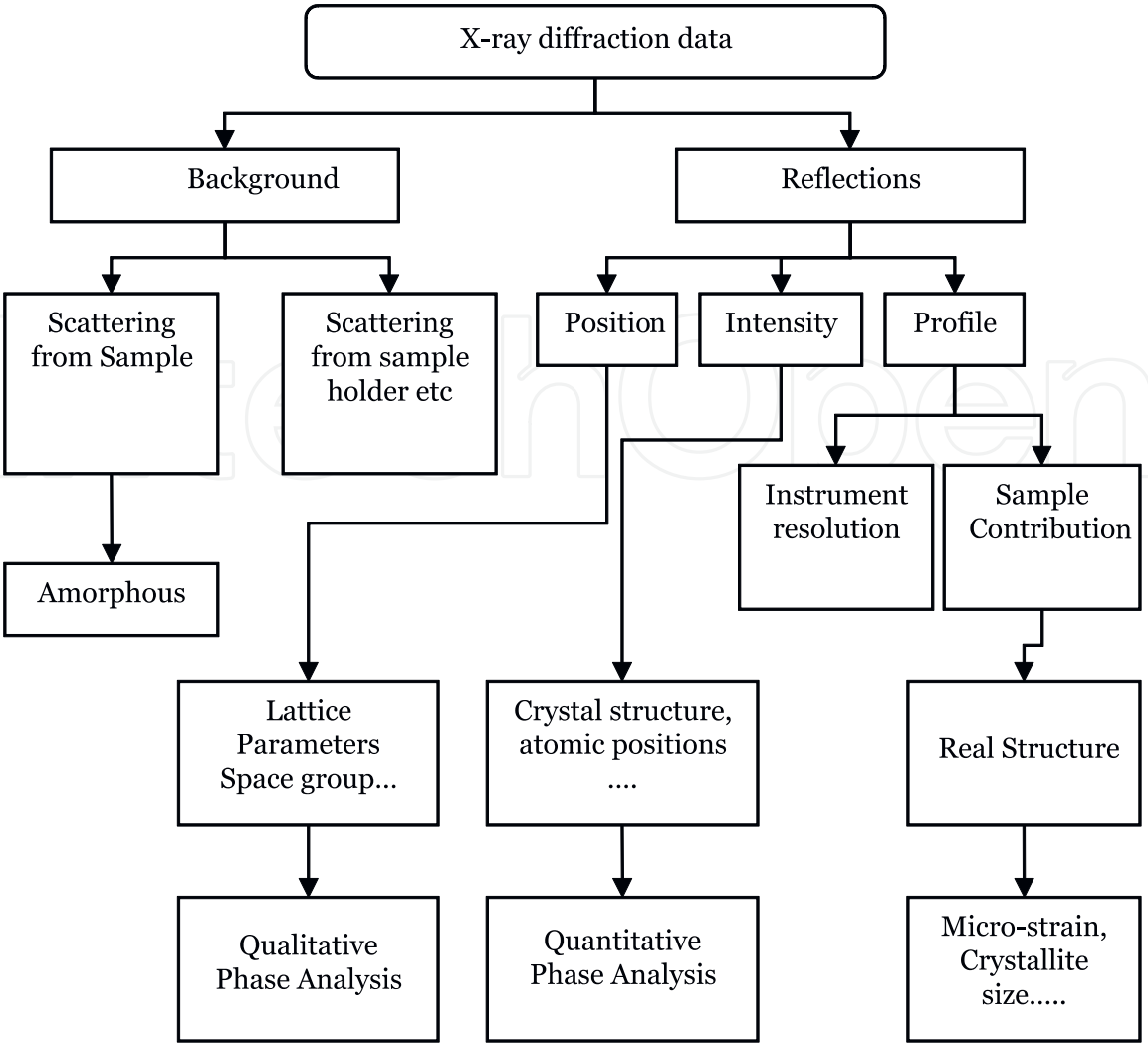


Figure 1.
The algorithm of whole profile refinement program developed by Hugo M Rietveld [reconstructed from the IUCr newsletter no. 26, Dec 2001].

current studies, antiquities and general information. This chapter attempts to accommodate most of these and present them in a more, newbie, newcomer friendly way. The chapter will follow a linear path from sample preparation, data collection to final results and conclusions accompanied by various current challenges, precautionary and explanatory notes.

3. Sample preparation

In order to understand different phases of sample preparation, we first need to define and understand the term “sample”. The term “sample” encompasses a much broader meaning in scientific community with or without any restriction on size, quantity, quality etc. A sample may be a rather large portion of material, or a very tiny amount. A specimen on the other hand is the representative diminutive piece of a sample. Although there is a thin line of distinction between a sample and a specimen in X-ray diffraction, the term sample preparation generally means to prepare a specimen from a larger sample [43, 44].

The material, phase purity, homogeneity, density gradient etc. of a sample from which a specimen is taken are to be considered in advance. For a phase pure sample or mostly pure, a specimen is a good representative of the sample, so is the case with multiphase but homogenous samples. However a specimen from a multiphase and

inhomogeneous sample may not be a good representative of the sample itself. The sample may consist of several phases, known or unknown, and may also include amorphous material. Depending on the technique and radiation, it may be small or large (neutron diffraction), it may be flat (Bragg–Brentano geometry), or cylindrical (Debye–Scherrer technique). In case of multiphase sample or amorphous contributions specimen should be taken with considerable representation of the sample such that during the refinement process quantitative contribution of each phase can be estimated more precisely.

In the length of this chapter the term “sample preparation” will be used to define collection of specimen, cleaning or remolding, mounting it on sample holder and all the processing necessary to prepare the diffracting material to its mounting on goniometer.

3.1 Precautionary/explanatory notes

Following few precautions are integral parts of sample preparation process

- Sample homogeneity/representative specimen
- Sample geometry
- Sample thickness
- Crystalline/Amorphous nature of sample
- Hygroscopic, gas absorbing nature and porosity of material
- Phase purity or at least the idea of chemical composition.

3.2 Current challenges

Despite the advances in current instrumentation and techniques we will not be able to obtain a 100% representative specimen from any sample, particularly powder samples. Grain size distribution, preferred orientation, inhomogeneous grain boundaries, defects and other microscopic differences will always act against it [45].

As world dives more and more into the nanoscale world, the sample thickness poses a problem with 1D and 2D materials.

Sample geometry can also not be obtained with certainty with nanoscale samples, especially with nano-morphologies and surface rough samples. A sample of 50–100 nm thickness and spiky morphology, with each spike of let us say 20 nm thickness and 50 nm length, will have so rough surface that there will be roughly 50% of thickness change while moving from one spike to another.

Another challenge will be the porosity of the samples. In nanomaterial samples the surface area to volume ratio increases leading to apparent amorphicity in actually crystalline samples.

4. Data collection

In order to perform a successful Rietveld refinement, it is essential that the powder diffraction data be collected appropriately. If relative intensities or the 2 θ values (d-spacing) are recorded incorrectly, no amount of time spent on refinement will lead to any sensible results. The factors to be considered for effective and

successful data collection are diffractometer geometry, instrument alignment, calibration, the radiation, the wavelength, slit size, necessary counting time and most importantly the alignment and positioning of incident beam [46].

It's important that the incident beam should always be kept on sample (specimen) such that the diffracting volume remains constant. In Bragg–Brentano configuration, the use of wide divergence slits must be accounted by a correction term. Introduction of this correction term is quite plainly geometry dependent, therefore, sample holder geometry has to be taken into consideration and an update to correction term should be applied. Most of the instruments correct this by using rotating circular sample, however, this does not always correct for low angle intensities. A more modern approach to this problem is the use of automated variable divergence slits which operate as a function of 2θ . At lower angles smaller slits are used, and at higher angles wider ones. A flat sample for Bragg–Brentano geometry is essential to ensure that focusing circle is always tangential to the sample surface. It is however practically more challenging to achieve surfaces with low roughness. At lower angles, the effect is negligible as the incident beam area is large, but at higher angles, as beam width decreases, the surface roughness can cause problems in collected data. A more common approach to this problem is to spend more time at collecting data at higher angles. Most of the modern diffractometers are equipped with such algorithms and generally adjust automatically as a function of θ . Next time you perform XRD measurements on your sample and find the higher 2θ data collection are getting on your nerves. Remember, it is for the best [47].

Time is also an important factor to consider while data collection [48]. It is necessary to record suitable counts; therefore more time should be spent between each 2θ step. It is also necessary to record the data at suitable intervals (step size) to ensure recording of good profile and peak-broadening. As a rule of thumb, there should be at least 5 data points collected across a given peak. The maximum 2θ should always be kept to as low as you can go, however at least 50 2θ degrees should be measured to ensure statistical viability of data.

Sample transparency is yet another problem. The assumption for XRD in reflection geometry is satisfied only when the sample is infinitely thick. If the sample contains only light elements, this condition might not get fulfilled at all, therefore all the following assumptions will be invalid [38, 48–50].

- i. The constant-volume assumption
- ii. The intensities measured at higher angles
- iii. The focusing circle adjustment etc. On the other hand, heavily absorbing samples can also be a problem, because the incident beam cannot penetrate the whole sample. The solution in the later case is much simpler than former one. Sample in later case may have to be diluted with a light-element material (e.g. diamond powder or glass beads).

Preferred-orientation effects can be very difficult to eliminate, especially for flat powder specimens. If the intensities show a strong hkl dependence (e.g. all hkl reflections are strong and all h00 weak), preferred orientation of the crystallites should be suspected. Rietveld refinement can be done with many programs which are based on March model allowing a specific crystallographic vector based refinement of preferred-orientation parameter [32]. The elimination (or minimization) of the problem experimentally is to be preferred due to the crude nature of such models. Grain and particle morphology can also play a major role in preferential orientation. For large crystallite size the randomness of orientation of sample gets diminished i.e.

not all crystallite orientations are equally represented, creating a problem. In the underrepresented specimen, the preferred orientation parameter cannot be corrected at the refinement stage. Therefore the sample rotation method is strongly recommended in such cases. In smaller particle sizes, line-broadening effects due to crystallite size begin to become apparent which evidently decreases the intensity of peaks. The presence of large crystallites within such samples will cause the peaks from smaller particle size to be relatively very low or even reduced to background. In such cases also, the correction to preferred orientation parameter cannot be applied.

Another parameter to be considered in the diffractometer is to keep background to maximum peak ratio as low as possible.

Monochromatic radiation is to be preferred for all XRD measurements. Although longer data-acquisition times are required with monochromatic radiation, its use is particularly advantageous both in number of lines and the background observed.

Any temptation to smooth the diffraction data before doing a Rietveld refinement must be resisted. Smoothing introduces point-to-point correlations which will give falsely lowered estimated standard deviations in the refinement process.

The wavelength and zero offset should be calibrated with a reference material. The Si SRM 640b standard gives significantly broadened peaks, whereas the NIST LaB6 standard SRM 660 gives close to instrumental resolution and is probably a better choice.

The example of over, normal and under collection of data is shown in **Figure 2 (a), (b) and (c)** respectively, while the presence of preferred orientation and normal XRD pattern of SnO_2 are shown in **Figure 3a and b** respectively.

4.1 Precautions and explanations

Specimen should be chosen in such a way that it represents the sample in every possible way (or at least nearly every way).

Uniform surface and thickness should be maintained across the sample.

In case of suspected preferred orientation, it should be a practice to repeat the experiment with newly prepared sample or specimen.

Many materials undergo phase transformation on exposure to humidity, Carbon Monoxide etc. In such cases, care should be taken to minimize the exposure.

Leveling of sample holder is essential to get an initial 2θ estimate.

In case of grazing incidence (GI) mode especially the background to peak height ratio is generally very low, therefore data collection is trickier. In order to minimize external errors thin film surfaces should be cleaned of any debris. Dust or other organic residues can sometimes reduce the quality of data by either hindering the path of beam or decreasing the intensity of peak recordings. This in some extreme cases can lead to inferences like oriented films, amorphous growth or preferred orientation errors.

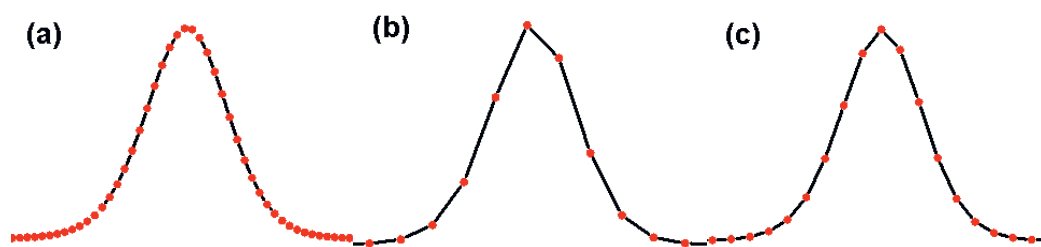


Figure 2.

The data (a) over collection (b) under collection (c) normal collection conditions for XRD data.

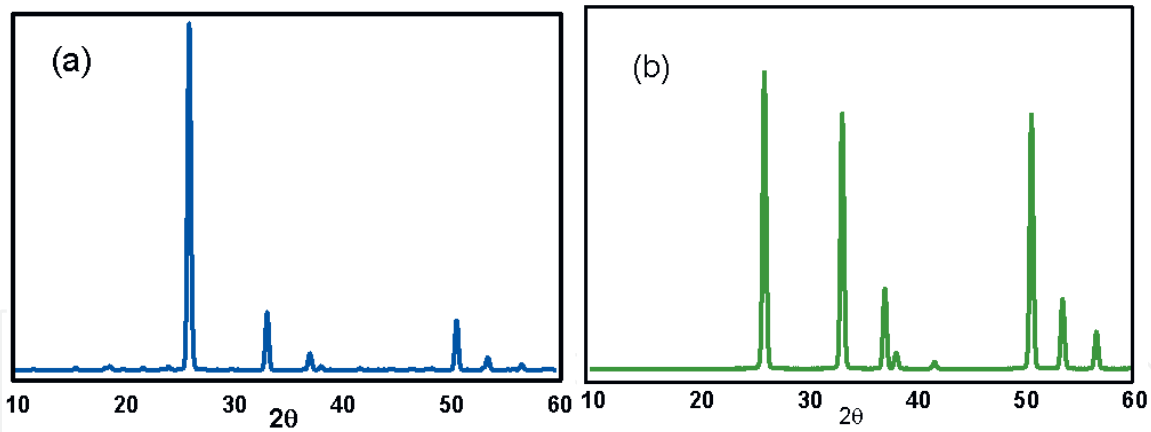


Figure 3.
SnO₂: (a) the observation of preferred orientation due to poor particle distribution while sample preparation (b) data collected after 2 hr. grinding.

4.2 Challenges

The continuous motion of either or both detector and source arms of goniometer and the recording transit time of the cameras are one of the bigger challenges modern x-ray diffractometers face. Although the introduction of step size has essentially eliminated this problem, there are still concerns regarding too close and too far step sizes. Both can affect the peak geometry and background contribution in more effectual way. Too close step sizes, lower symmetry phases/peak splitting are bad combinations. Wide step sizes and nano-materials/GI mode/multiphase samples are also bad combinations. The time dependence of step size choice and effective counting times are the current limiting factors for diffractometers.

5. Background contribution

As discussed in previous section, the data collection should essentially be optimized to obtain least background. However, in practicality there are many possible unavoidable, yet necessary and characteristic reasons where background cannot be minimized after a certain degree without degradation of peak data quality. Although for pure phase materials, the background essentially remains negligible, till the particle or crystallite sizes are greater than 100 nm and grain boundaries are insignificant. For multiphase materials, the relative intensity difference between the peaks of different phases due to preferred orientation, crystallite size difference, peak broadening, quantitative presence, and sometimes amorphous phase do make background contributions a part of the X-ray reflection geometry [51].

Basically, the background contributions are dealt in two different ways in a powder diffraction pattern. Background can be modeled by an empirical/semi-empirical polynomial function with several refinable parameters or it can be estimated and at the end subtracted by a linearly interpolated set of points. Background subtraction although seems inelegant, is more sophisticated in circumstances where polynomial function cannot describe the background well. The normal procedure for background estimation should be an initial estimation using polynomial function, followed by (if required) linear interpolation and subtraction. This method is supposed to both preserve the estimates of standard deviations and correct for the background contribution optimally. It should also be noted that if a polynomial function does not describe the background well, no amount of refinement of its

coefficients or increase in its order can fix the problem. In such cases for a complete and satisfactory refinement process, the estimation of background should be skipped and linear interpolation and subtraction procedure should be followed. While background is generally eliminated in refinement process, the peak base shapes are essentially a part of background and therefore at higher 2θ , more care should be taken in estimating the background. This is why background fitting using linear interpolation by cubic-splines should be generally avoided. The asymmetric peak shape especially at higher 2θ (where peak intensities are generally low) and non-careful background estimation or subtraction can affect the relative intensity of peaks and therefore degrade the overall refinement quality.

Figure 4(a), (b) and (c) respectively show contribution of amorphous, nanoscale and micrometer-scale phase towards background in LaMnO_3 samples.

5.1 Precautions/explanations

More time spent on measurement less significant background. This is somewhat misleading the background does not actually change with increased time spent per step. It is the increase in the number and intensity of counts per peak that increases which visibly smoothens the background. The precautions for background contribution during data collection have been discussed previously are almost entirely

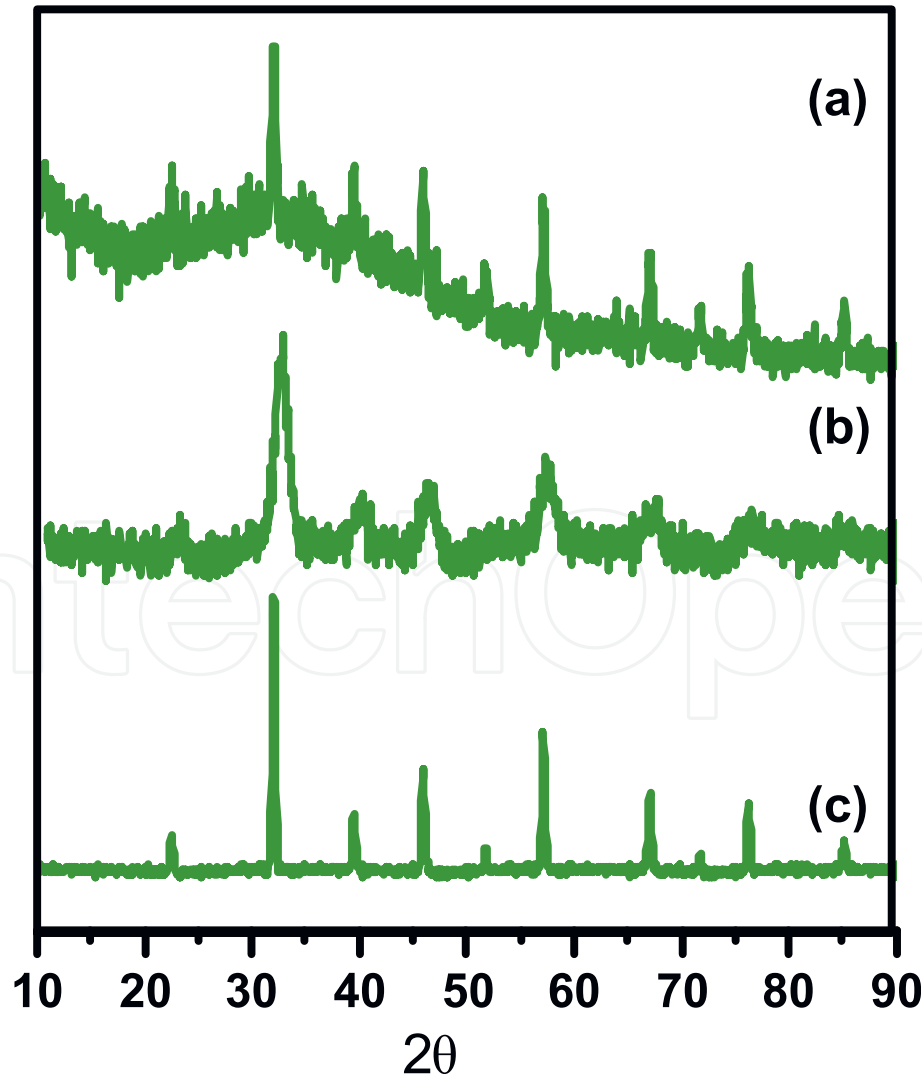


Figure 4. XRD pattern for (a) mostly amorphous, (b) nanoscale and (c) micrometer-scale phase of LaMnO_3 . The hump visible in (a) is a characteristic of amorphous phase, while the noisy background in (b) is characteristic of nanoscale phase due to low intensity counts.

complete set. During refinement and background estimation/subtraction, precautions need to be taken for segregating peak bases from background.

5.2 Current challenges

We are essentially in a nano-technological world right now and most of the materials applications around us have transitioned from bulk to micro to nanoscale. The complexities associated with the nanoscale XRD have also risen noticeably [52–55]. Nanoscale background contribution, irregular peak shapes, non-correctable preferred orientation/asymmetry parameters, sometimes odd combination of Lorentzian and Gaussian peak parameters. The porosity and reduced dimensionality (especially, 1D, 2D materials) are very difficult to characterize via normal XRD procedures.

6. Peak-shape function

The peak shape is one of the most important parameters in Rietveld refinement due to its dependence on crystallite/domain size, stress/strain, defects/vacancies, source/geometry, slit-size/detector resolution and $2\theta/hkl$ indices [55]. An accurate description of the shapes of the peaks in a powder pattern is critical to the success of a Rietveld refinement. Poor description can lead to unsatisfactory refinement results, false minima and divergence. Peak shape analysis/function is the most complex parameter in Rietveld refinement, with dimensions into the space of unattainable and non-realistic. It is therefore essential for a working algorithm to make some assumptions/compromises on peak shape and sometimes neglect the otherwise essential aspect of peak shape. For x-ray and constant wavelength neutron data, the use of pseudo-Voigt approximated peak function is widely used. The pseudo-Voigt function is essentially a combination of Lorentzian and Gaussian peak function in a linear mode [30, 31, 56–61].

Voigt function is mathematically defined as

$$V(x, p, y) = \int_{-\infty}^{+\infty} G(x, p) L(x - x', y) dx' \quad (1)$$

Where $G = \frac{e^{-x^2/2p^2}}{p\sqrt{2\pi}}$ is Gaussian function and $L = \frac{y}{\pi(x^2 + y^2)^m}$ is Lorentzian function with $m = 1$ for symmetry.

The pseudo-Voigt function is described as

$$V_p(x, f) = \eta L(x, f) + (1 - \eta) G(x, f) \quad (2)$$

With

$$0 < \eta < 1$$

η is the full width half maximum parameter and the ratio of Gaussian and Lorentzian functions $\eta/(1 - \eta)$ determines the mixing of these functions.

The graphical representation of the pseudo-Voigt function with variable η is shown in **Figure 5**.

Pearson VII peak-shape function (**Figure 6**) is used alternatively where the exponent m (Eq. 1) varies differently, but the same trends in line shape are observed. Although the Gaussian and Lorentzian components of Voigt function can be devolved into meaningful physical interpretations of stress/strain, microstructure and line broadening effects, no such interpretation can be drawn from Pearson

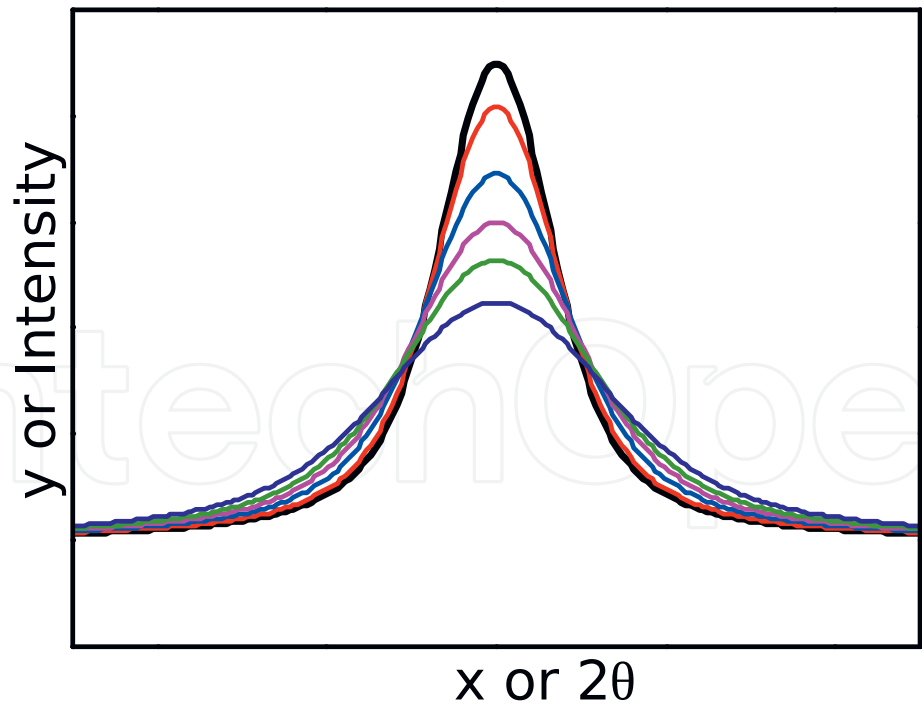


Figure 5.
Pseudo-Voigt peak function (black) and variation of peak shape (color) with η .

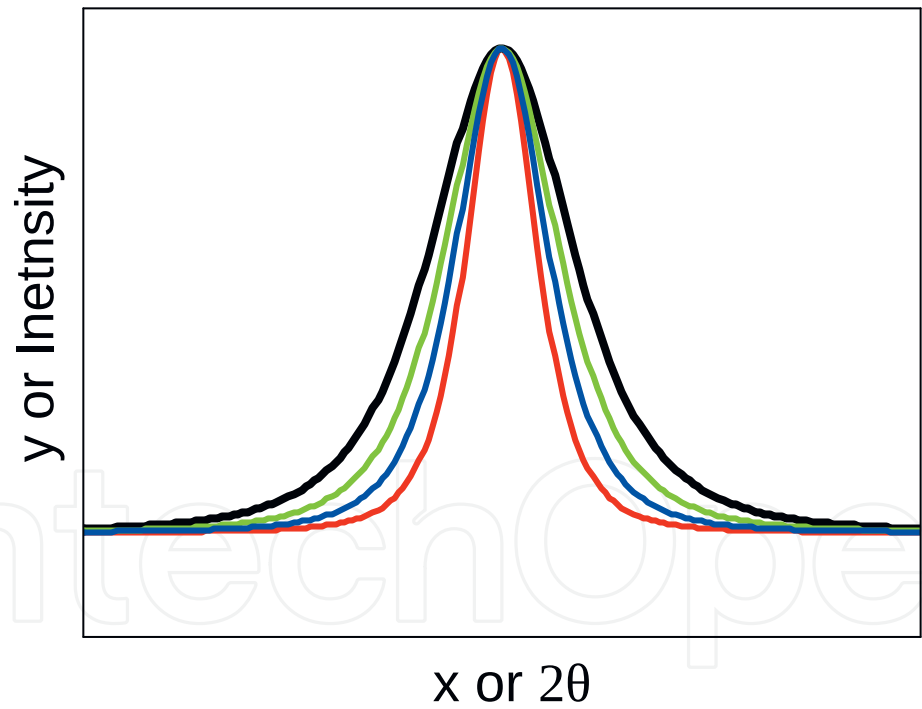


Figure 6.
Pearson VII peak function (black) and variation of peak shape (color) with m .

VII function. Another advantage of pseudo-Voigt peak function over other functions is the separation of sample and instrument contributions.

$$I = I_o \frac{y^{2m}}{\left(y^2 + (x - x')^2\right)^m} \tag{3}$$

It is also imperative to point out that pseudo-Voigt peak fitting accounts for peak base asymmetry more rigorously while Pearson VII is more inclined towards the peak

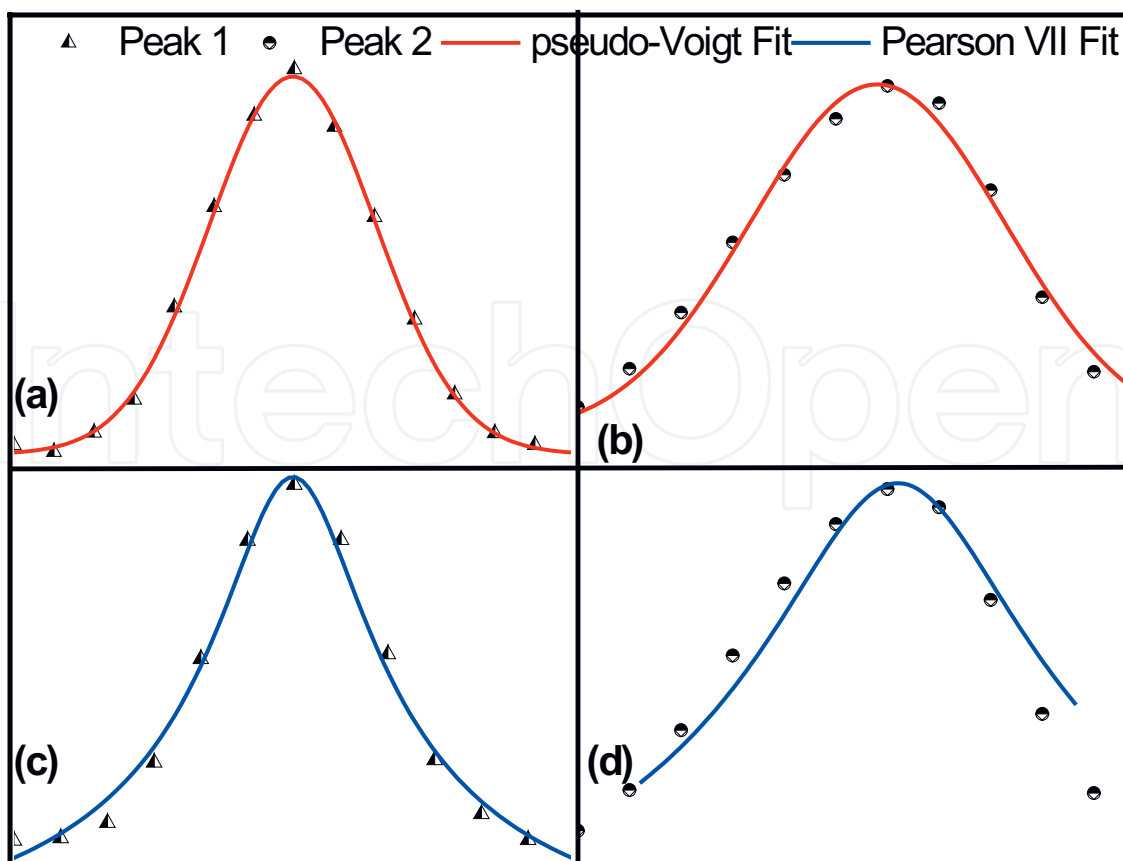


Figure 7.
 Variation of fitting between two different shapes of peaks (triangles and circles) using (a), (b) pseudo-Voigt (red) and (c), (d) Pearson VII function (blue).

centre and Intensity offset. The property of these peak functions can be employed more efficiently by empirical evaluation of the peak shapes. Although both the functions provide similar results when the variation of peak shapes with 2θ is accounted.

The variation in chi-square fitting ($\chi^2 \sim 0.01$) of peak and base in both pseudo-Voigt and Pearson VII function can be visualized in **Figure 7(a)-(d)**.

7. Profile parameters

The profile parameters include every detail that a structural model packs in, except (background, peak shape and FWHM). Although FWHM is considered a part of profile in XRD, it is necessarily a variant under peak shape function. Therefore most of the available programs for Rietveld refinement list it under profile section. Practically, Clubbing of the asymmetry parameter, preferred orientation parameter and FWHM together due to their interdependence makes more sense. The structural model which is available should be complete otherwise the calculated profile will significantly deviate. The incorrect profile parameters during refinement process generally leads to refinement of FWHM, peak asymmetry, zero shift, etc. In such cases, it is more prudent to use methods that are structure independent. Le-Bail [23, 39, 62–65], Pawley [66, 67] etc. are suitable for obtaining initial values of profile parameters and extract a list of integrated intensities. The integrated intensities can then be used to calculate electron scattering densities and possible structure determination. In addition, the initial parameters can be refined to obtain more agreeable profile parameters. The information like crystallite size, defect concentration, microstrain etc. which can be extracted from XRD are derived from the profile

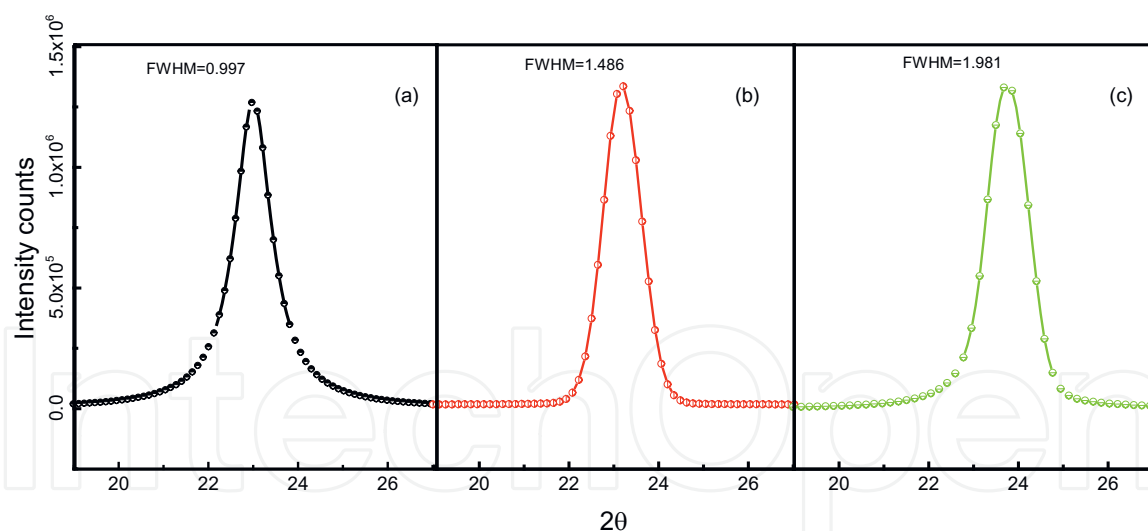


Figure 8.

The interplay of peak width, shape and its effect on FWHM with (a) symmetric profile (b) asymmetric profile without significant peak shift and (c) asymmetric profile resulting in significant peak shifting.

parameters. Although, the independence of profile parameters and peak shape is questionable due to their correlated nature, to make physical sense from the variation of either, the profile parameter needs a separate part in X-ray diffraction. The asymmetry in peak profile is another feature that arises from convolution of closely spaced multiple peaks. The two common and prevalent reasons for such conditions are; the evolution of microstrain and the defects. However the contributions from the instrument and the sample holder cannot be undermined. The interplay between FWHM, Peak position, shape and width is best visualized graphically (**Figure 8**).

7.1 Precautionary/explanatory notes

Although the basic idea about chemical composition, cell volume and density are needed to obtain a solution to an unknown phase, search using Le Bail, Pawley or ITO, DICVOL, TEROR, EXPO can always be widened to obtain initial profile parameters. However lower symmetry crystal systems like monoclinic and triclinic should not be included unnecessarily. These programs are likely to give multiple solutions to single set of reflection and it remains up to the user's judgment in these cases to choose a suitable solution. The multiple solutions are more prominent when lower symmetry systems are included, and sometimes the search criteria need to be adjusted to remove unrealistic solutions. In general, unrealistic solutions tend to possess either of the characteristics listed below or their combination:

- i. Very large/small cell volume
- ii. One or more of the cell parameters in extremely large/small¹
- iii. The fractional atomic coordinates are unrealistic
- iv. The number of atoms per unit cell are either very high or low
- v. Atomic overlapping

¹ The case of rhombohedral symmetry which is generally expressed in hexagonal axes format should be treated individually. It is normal in some materials which crystallize in rhombohedral symmetry to have large 'c/a' ratio when expressed in hexagonal axes. Few of the examples are Telurides, Selenides and lannonites.

8. Rietveld refinement: procedure and guidelines

After getting a complete structural model, suitable unit-cell parameters, the sufficient profile parameters and agreeable background, the Rietveld refinement of structural parameters can be started [68–71]. Refinement is usually done in sets of two to five cycles at a time but for effective refinements in simpler crystal systems hundreds of cycles will be required and thousands for complex systems. While the refinement is underway, we can monitor the progress either graphically or numerically [49]. While the numerical parameters can give us a statistical idea about the refinement, the most useful information about the profile fit is best seen graphically. However the parameter shifts are much more rigorously visualized numerically. Introduction of Reliability factors or R values by Rietveld enabled us to visualize profile fit between observed and calculated patterns more effectively, although the graphical inspections still retain their superiority. The difference plot is also a good indication of the quality of profile fit, however the actual difference between the observed and calculated profiles and the origination of the deviation is not always quite evident from it. **Figure 9** shows the full profile Rietveld refinement of LaMnO_3 (couple more example of Rietveld refinement are given at the end of the chapter) while **Figure 10** shows the observed and calculated profile for a certain peak along with difference plots, while the corresponding R values for the whole profile are listed in the table. The increased R-values can be due to insufficient structural model, or inaccurate profile parameter. The atomic coordinates and positional parameters can cause changes in relative peak intensities at both high and low angles. The refinement of all the parameters has to be either done simultaneously or in a particular order to avoid numerical and statistical errors. The order and the explanation of the various refinable parameters and reliability factors will be done

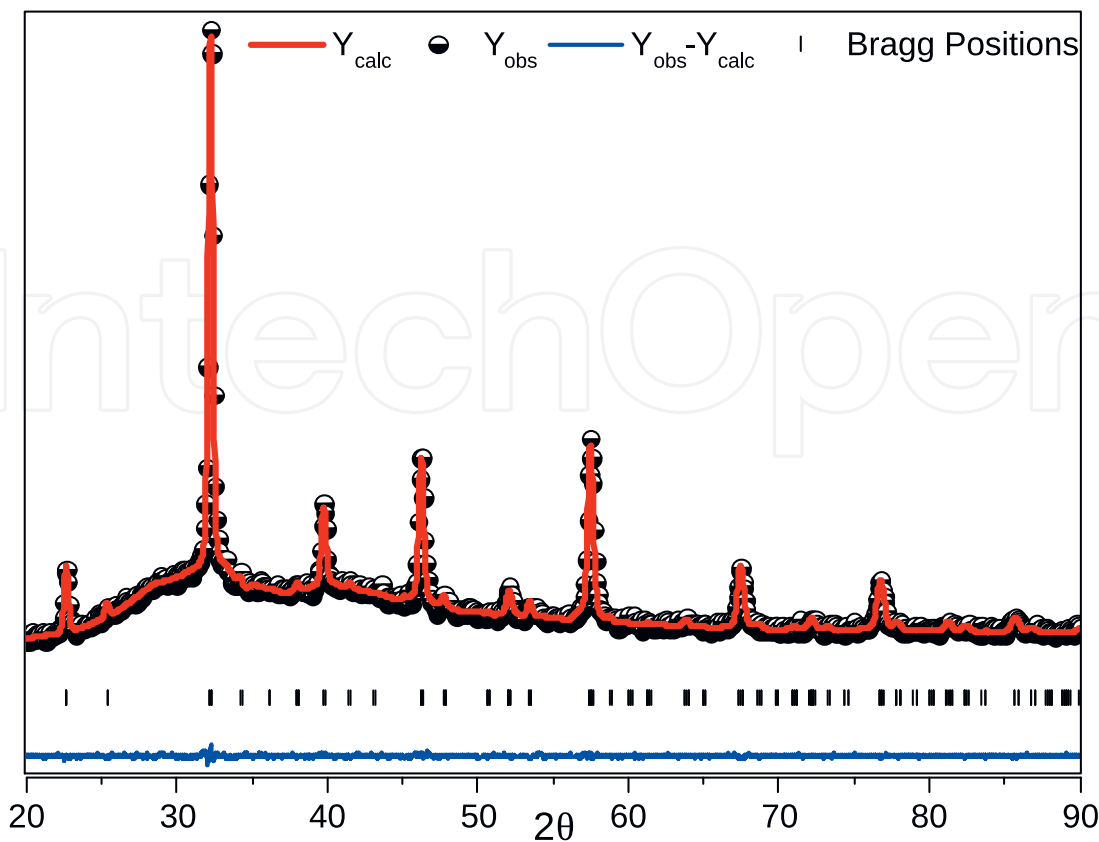


Figure 9.
Typical Rietveld refinement plot (LaMnO_3) with observed (black circles), calculated (red), difference (blue) and Bragg positions (black bars).

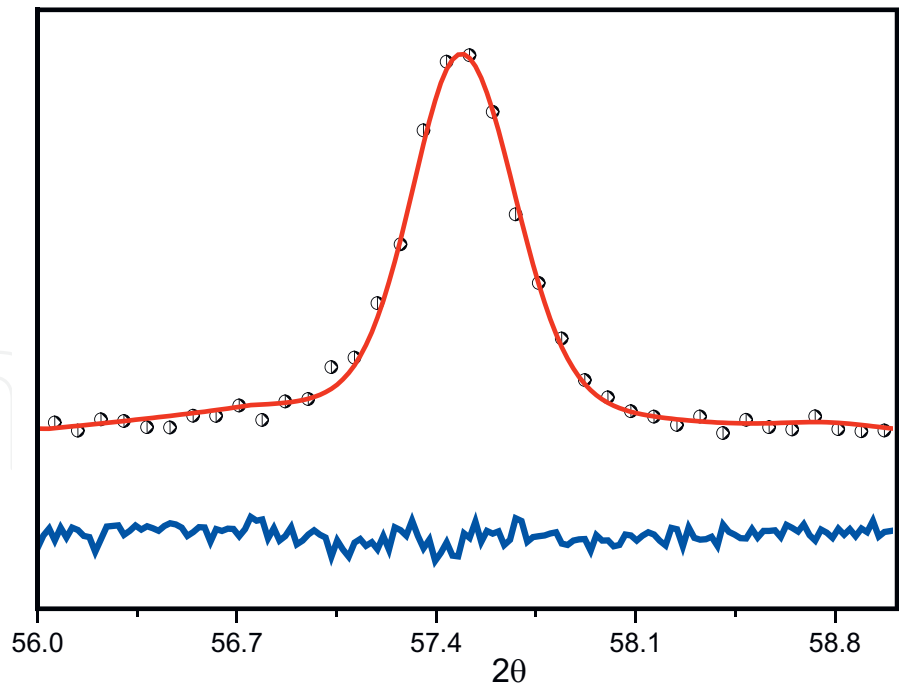


Figure 10.
The zoomed in view of peak at around 57° from **Figure 9** to visualize the goodness of fit.

in later sections. It is important to know the source of errors in the refinement procedure for a effective and concise results. The most common error that occurs is due to the noisy data. The noisier the data the more refinement is needed for background parameter, this can sometimes lead to convolution of peak bases into background especially at higher angles. Zero shift and sometimes step size can also cause a range of errors to creep in. it is therefore a common procedure to first correct the data for zero shift and choose a more incredulous step size at the time of data collection. Apart from these, we need to look out for most of the other errors while the refinement process is underway. Sometimes lower estimated standard deviations can result from false minima observed due to unavailability of suitable structural model or unrealistic positional parameters (**Table 1**) [42, 43].

9. Refinement procedure

It is difficult to cover all the details of a full refinement, but an approximate strategy can be described. It is generally advised to begin the structural refinement first with the positions of the heavier atoms and then extend the refinement to positions of lighter atoms. It should however be always kept in mind that the statistical minima can sometimes attribute unrealistic positions to the atoms. All atomic positions, with constraints in place, can be refined simultaneously upon convergence. The scale, the thermal and the occupancy parameters are more

χ^2	R_{wp}	R_{exp}	R_F	R_{Bragg}
1.25	2.65	2.11	2.29	3.58

Table 1.
The chi (goodness of fit), and other Rietveld reliability factors (explanation of each factor in “R-factor” section ahead).

sensitive to the background correction due to their correlated nature. Positional parameters are somewhat independent of background. In order to reduce the number of thermal parameters to be refined in early stage, it is advisable to constrain the thermal parameters of similar atoms. Chemical constraints should be applied to maintain the physical sense of occupancy parameters. Refining a single structure using two independent data-sets e.g. x-rays and neutron diffraction the parameter correlation can be minimized. However, the experimental conditions for data collections such as pressure, temperature etc. in each case should be as similar as possible. Refinement of the profile parameters along with the structural parameters is also advisable. The structural model should be refined to convergence while care should be taken to retain the physical and chemical sense wherever applicable. Mere convergence with even a single parameter not making physical or chemical sense is all the efforts wasted. It is therefore necessary to always follow a certain procedure/pathway of refinement or at least at the earlier stages of refinement. The likely procedure of refinement pathway is given in **Figure 11**.

Because powder diffraction data are a one-dimensional projection of three-dimensional data, the inherent loss of information is always a problem. To partly compensate for this loss geometric information (bond distances and/or angles) taken from related structures is more appropriate method. The purpose of these constraints is to increase the number of observations by added geometric conditions. Another way to implement restraints is to follow rigid body model, this however results in decrease in the number of observations and complicating the structural model. The use of geometric restrains not only increases the number of observations but allows more parameters to be refined, while keeping the geometry of the structural model sensible. The set of geometric restraints can be treated as separate data set, with same rules of quantity minimization in the refinement. The geometric data set can be represented as:

$$S = S_y + c_w S_G \quad (4)$$

where S_y is the weighted difference between the observed [$y (obs)$] and calculated [$y (calc)$] diffraction patterns,

$$S_y = \sum_i w_i [y_i(obs) - y_i(calc)]^2 \quad (5)$$

S_G is the weighted difference between the prescribed [$G(obs)$] and calculated [$G(calc)$] geometric restraints,

$$S_G = \sum w [G(obs) - G(calc)]^2 \quad (6)$$

and c_w is a factor that allows a weighting of the geometric observations 'data-set' with respect to the diffraction data-set.

Geometric restraints can enhance a refinement considerably, allowing otherwise impossibly complex structures to be refined successfully. However care must to choose the bond distance and angles in order to accommodate the appropriate polyhedral geometry. It is imperative that the final structure model should fit both the geometric and the X-ray data satisfactorily.

9.1 Quantitative refinement

The methodology involved in qualitative and quantitative Rietveld refinements have been discussed at length by many authors [26, 27, 49, 72]. The theory behind

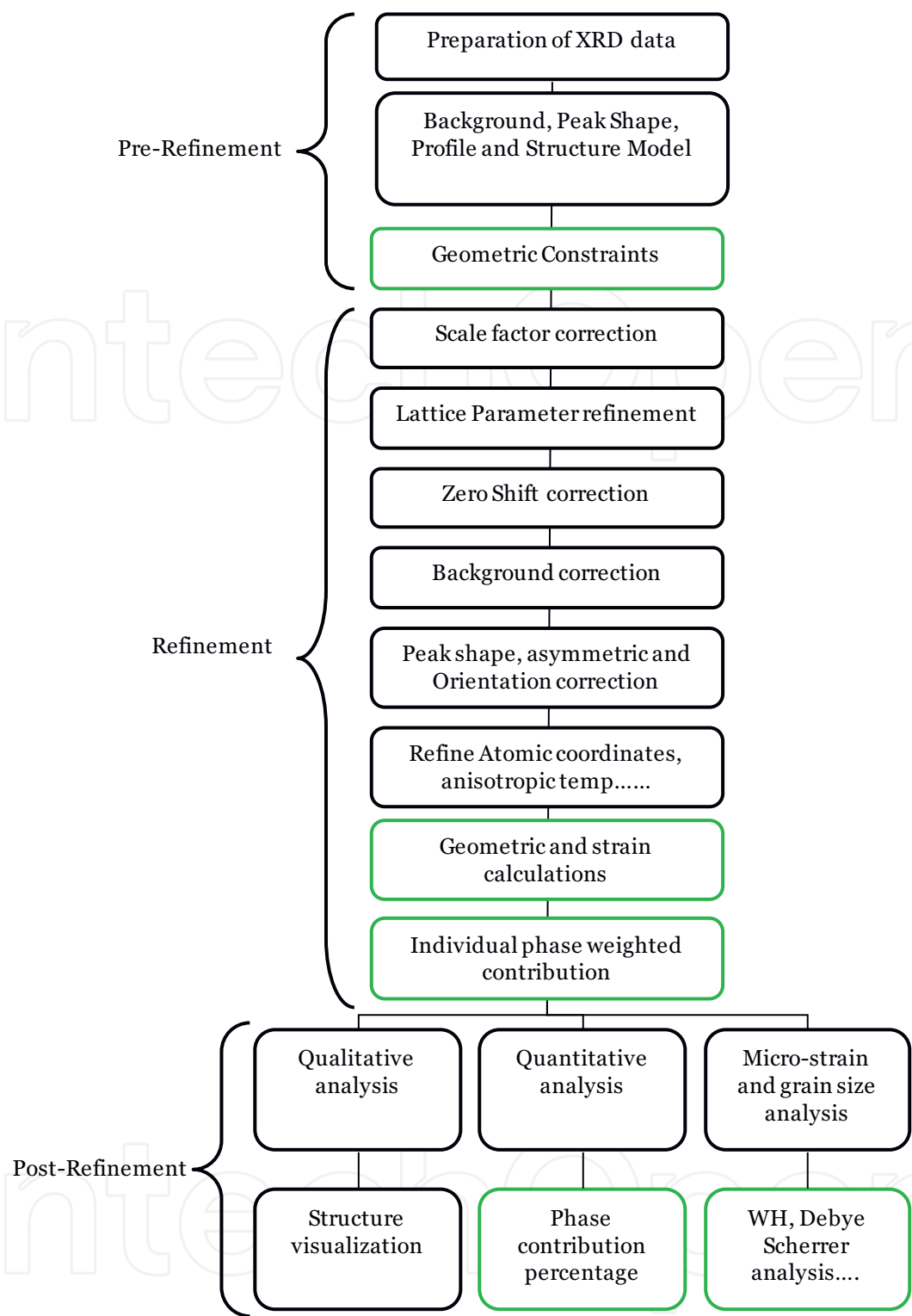


Figure 11.
The procedure typically followed during the refinement of XRD data via Rietveld method. The green boxes are optional calculations. The variation of procedure is necessary in cases with amorphous phases, anomalous reflections or sample induced asymmetry.

Rietveld quantitative analysis is identical to that implemented in most conventional quantitative analyses [34, 73–76]. The integrated intensity of X-rays diffracted by a randomly oriented infinitely thick [40, 76–81] polycrystalline sample in flat-plate geometry can be written for a particular reflection as:

$$I_{hkl} = K(1/2\mu)R_{hkl} \tag{7}$$

Where K and R_{hkl} are the hkl invariant and variant parameters.

The detailed discussion of the mathematical and physical interpretations of these quantities can be found abundantly in literature, particularly in the cited works [72, 82–84].

In a mixture, the intensity of hkl reflection originating from a particular phase (α) is written as

$$I_{\alpha,hkl} = C_{\alpha} K \left(\frac{1}{2\mu_m} \right) R_{\alpha,hkl} \quad (8)$$

Where C_{α} is the volume fraction of α phase with μ_m as linear absorption coefficient. In terms of weight fractions, which is statistically more convenient, the equation can be written as

$$I_{\alpha,hkl} = \frac{W_{\alpha}}{\rho_{\alpha}} K \frac{\rho_m}{2\mu_m} R_{\alpha,hkl} \quad (9)$$

Now the scale factor for alpha phase can be written as

$$S_{\alpha} = \frac{W_{\alpha}}{\rho_{\alpha}} K \frac{\rho_m}{2\mu_m} \quad (10)$$

For second phase (β), the weight fraction can be done similarly while the net contribution per phase can be sought from the equation below

$$W_{\alpha} = \frac{W_{\alpha}}{W_{\alpha} + W_{\beta}} \quad (11)$$

The equation can be solved by replacing weight fractions by equation above

$$W_{\alpha} = \frac{S_{\alpha} S_{\beta}}{S_{\alpha} \rho_{\alpha} + S_{\beta} \rho_{\beta}} \quad (12)$$

As scale parameters are refined we will get estimated weight fraction contribution of each phase.

9.2 R values

The numerical way of observing the quality/goodness of fit, although not as prudent as graphical visualization of difference plots, provides a good, intuitive numerical estimate. This is usually done in terms of agreement indices also called Residual values or Rietveld refinement indices or Rietveld discrepancy indices or R values [26, 27, 85–87] which are expressed as.

9.2.1 The weighted-profile R-value

The weighted profile R values (R_{wp}) is most straight forward and follows directly from the square root of minimized quantity, scaled using weighted intensities and is defined as:

$$R_{wp} = \left\{ \frac{\sum_i w_i [y_i(obs) - y_i(calc)]^2}{\sum_i w_i [y_i(obs)]^2} \right\}^{1/2} \quad (13)$$

where $y_i(obs)$ is the observed intensity, $y_i(calc)$ the calculated intensity, and w_i the weight at i^{th} step.

The numerator in Eq. (13) is the expression that is minimized during a Rietveld refinement procedure. Thus the inclusion or exclusion of background can have dramatic effect on the refinement. If the background has been excluded, and thus subtracted prior to refinement then, $y_i(obs)$ is the net intensity. However, the inclusion of background means the refinement of background parameters. In such cases, $y_i(obs)$ includes both background and net intensity. Therefore, $y_i(obs)$ and $y_i(calc)$ both will likely include the background contribution. In the latter case when dealing with a high background to peak intensity ratio, most of intensity will be attributed to background, resulting in lowered value of R_{wp} . Therefore it is recommended to subtract background in such cases. R_{wp} for laboratory X-ray data are large $\sim 10\%$. This is primarily due to the level of the background. In any publication, the type of agreement index used must be clearly specified. Ideally, the final R_{wp} should approach the statistically expected R value or R_{exp} .

9.2.2 The expected R -value

R_{exp} reflects both the quality of data and refinement and is expressed as

$$R_{exp} = \left\{ (N - P) / \sum_i w_i [y_i(obs)]^2 \right\}^{1/2} \quad (14)$$

where N is the number of observations and P the number of parameters.

However, the ratio between the R_{wp} and R_{exp} , called goodness of fit (χ^2), which is quoted quite often in the literature, should approach 1.

$$G^2 = \chi^2 = R_{wp} / R_{exp} \quad (15)$$

Most of the statistical errors in these R values can occur either due to under-collection or over-collection of data. The ratio will be less than one if data is under collected as R_{exp} will be much higher than R_{wp} . In case of over-collection the ratio will be greater than 1. It is always recommended to have over-collected rather than under-collected data. As estimated standard deviations [88] can also alter the ratio, there are other R values like R_F and R_{Bragg} which will improve the conclusivity of the data.

9.2.3 The structure factor R value

An R value based on structure factors, F_{hkl} , can also be calculated by distributing the intensities of the overlapping reflections according to the structural model.

$$R_F = \sum_{hkl} |F_{hkl}(obs) - F_{hkl}(calc)| / \sum_{hkl} |F_{hkl}(obs)| \quad (16)$$

R_F a derivative of structure factors is essentially biased towards the structural model. It can however give a clear indication of the reliability of structural refinement. Although not used actively while reporting the refinement of structure, it should necessarily decrease as the structural model improves in the course of the refinement.

9.2.4 The Bragg intensity R value

The Bragg-intensity R value (R_B) is essentially the structure factor R_F but in terms of Intensity I_{hkl} :

$$R_B = \frac{\sum_{hkl} |I_{hkl}(obs) - I_{hkl}(calc)|}{\sum_{hkl} |I_{hkl}(obs)|} \quad (17)$$

Where $I_{hkl} = mF_{hkl}^2$, m is multiplicity.

R values are useful indicators for the evaluation of a refinement, especially in the case of small improvements to the model which are not generally visible in difference plots. However, care should be taken while evaluating the R values as they are prone to over-interpretation. The most important questions that need to be asked for judging the quality of a Rietveld refinement are

- i. Is the fit between observed data and calculated pattern good?
- ii. Does the structural model make chemical sense?
- iii. Are inter-atomic distances and angles realistic?
- iv. Are the results from the refinement consistent with results from Raman, IR NMR etc. characterizations?

9.3 Common problems during refinement

Each structure refinement has its own idiosyncrasies and will present problems that require imaginative and selective solutions. However, some problems are of a more general nature and arise in many cases.

The most frequent source of difficulty in a Rietveld refinement is error in the input file. Most of these errors if occurring due to format or syntax can be corrected by conversion of files into suitable format using software like PowDLL from University of Ioannina.

The background does not seem to fit well

- i. Try a different background function, increase the number co-efficient, change from linear to polynomial or vice versa [19]
- ii. Try background subtraction
- iii. Try combination of (i) and (ii)

The peak shapes are not suitably fitting

- i. Check the difference plot and match with the **Figures 12(a)-(c)** to see if one of the characteristic difference profiles is shown. The respective profile parameter should be reset or further refined [20, 21]
- ii. Use a different peak-shape function
- iii. Perform asymmetry correction to the peak-shape function.
- iv. Line broadening and shifting along with 2θ dependence of FWHM can indicate microstructure contributions [89–91].

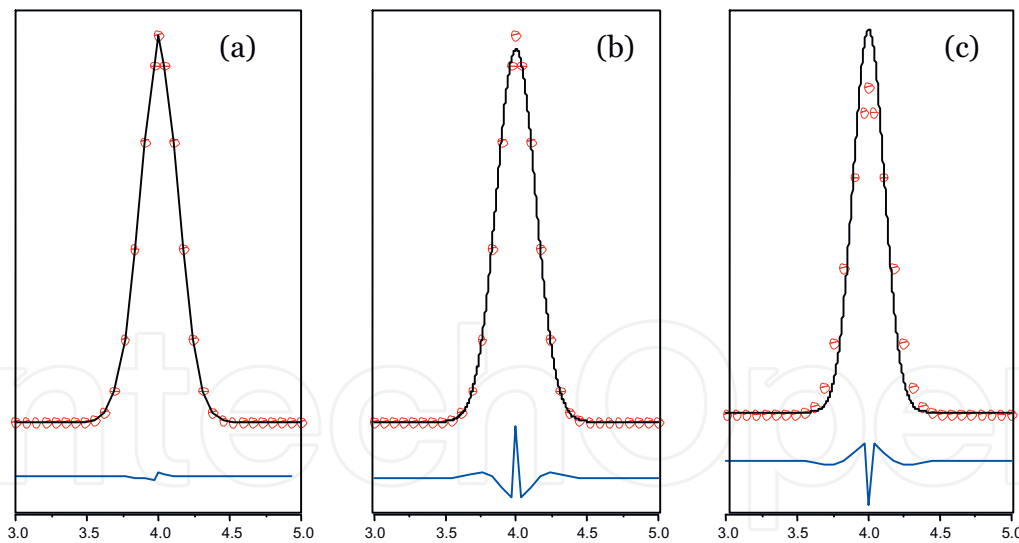


Figure 12.

(a) a good peak fit (b) Observed intensities are higher than calculated and (c) Observed intensities are lower than calculated (in both cases, possibly any of these might require to be reset or further refinement, (i) scale factor, (ii) preferred orientation, (iii) lattice parameters).

The peak positions in the calculated and observed patterns do not match

- i. Check if unit cell parameters are correct
- ii. Perform Zero shift refinement
- iii. Determine the unit-cell parameters via independent indexing methods

The tails of the peaks in the calculated pattern are cut off prematurely

- i. Increase the peak range used in the calculation

The relative intensities of a few reflections are high with very few low peaks

- i. This is usually indicative of rock in dust problem concerned with poor particle statistics. The only solution is to recollect the data after proper sample preparation

There multiple un-indexed peaks in the diffraction pattern

- i. Check for sample impurity
- ii. Check whether the infinite sample thickness condition was fulfilled during data collection
- iii. Check for peaks from sample holder

The refinement does not converge

- i. Look at the observed/calculated profiles carefully and check these.
 - a. Are the observed peak shapes well defined by peak shape function?
 - b. Is there any mismatch between peak positions?

- c. Is background refinement realistic and sensible?
- d. Is the scale factor correct?
- ii. Has structural model been completely described?
- iii. Check for oscillations in the parameter shifts and apply damping factors as. Most modern refinement software perform this automatically
- iv. Do not refine two parameters with high correlation together. Sometimes the high correlation is an indication of wrong space group
- v. Refine fewer parameters initially
- vi. Add geometric restraints
- vii. If geometric restraints are already in use, are they correct?
- viii. Fix thermal (atomic displacement) parameters at certain sensible values
- ix. Use a different space group.
- x. The number of parameters being refined is higher than what data can provide

The final structure is not chemically sensible (unrealistic inter-atomic distances)

- i. Use restraints to keep inter-atomic distance sensible.
- ii. Delete the offending atoms and try relocating them using Fourier maps [54, 59, 92, 93]
- iii. Change restraints [94]
- iv. Change the space group
- v. Fix atomic thermal displacements and fractional coordinates in the beginning

Refinement converged but there are few peaks which are not fitted well

- i. Check for Lorentz–polarization correction
- ii. Apply absorption correction parameter if data permits [95]?
- iii. Are atomic fractional co-ordinates correct?
- iv. Is there preferred orientation in the sample?

10. Structural visualization

The most important aspect of a Rietveld analysis is the refinement of structure. The actual structure of the sample can be calculated taking into consideration the

lattice parameter variations, the microstructure, stress strain contribution and other contributions. Effectively most of the currently available software for Rietveld refinement can easily generate the refined structure file. Visualization of structure at higher resolution has become easy with enhanced computational power. However the presentation of the structure is not standardized and most of the time the axial orientation is not mentioned. Although, it is not essentially a problem for the readers, the standard representation of the structure should be preferred. In cases where a non-standard representation is used, mention of plane, axial orientation, etc. should be clearly mentioned [90, 96]. The non standard representation of the structure can sometimes lead to wrong conclusions as shown in **Figure 13** for ZnO.

Apart from the problems discussed above, the tetrahedral and octahedral geometry should be visualized carefully (**Figure 14**). The actual polyhedral tilting, rotations or other geometric variations can be truly visualized only after symmetrised unit cell representation [97–99]. The **Figure 15(a)** and **(b)** show ZnO structure in symmetrised and non-symmetrised form. The difference in visualization is quite amazing [34, 100, 101].

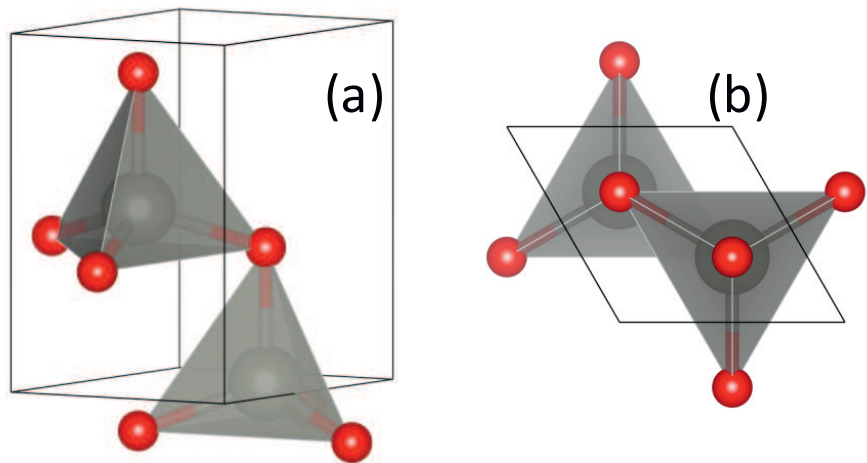


Figure 13.
(a) The standard view and (b) c^* axial view of hexagonal ZnO (●-Zn and ●-O) unit cell with non-standardized atomic positions.

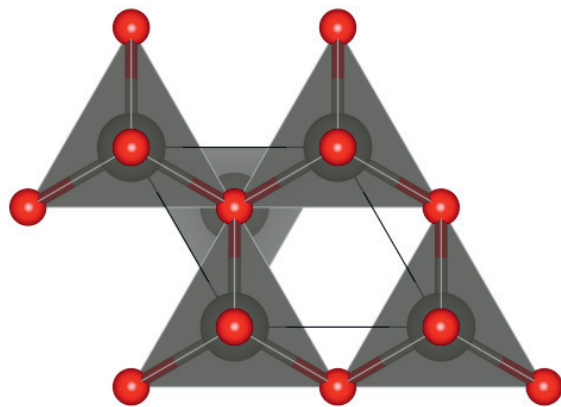


Figure 14.
The c^* axial view of hexagonal ZnO unit cell with standardized atomic positions. The transformation of structure to represent the hexagonal arrangement of ●-Zn and ●-O atoms is effectively visible within a single unit cell.

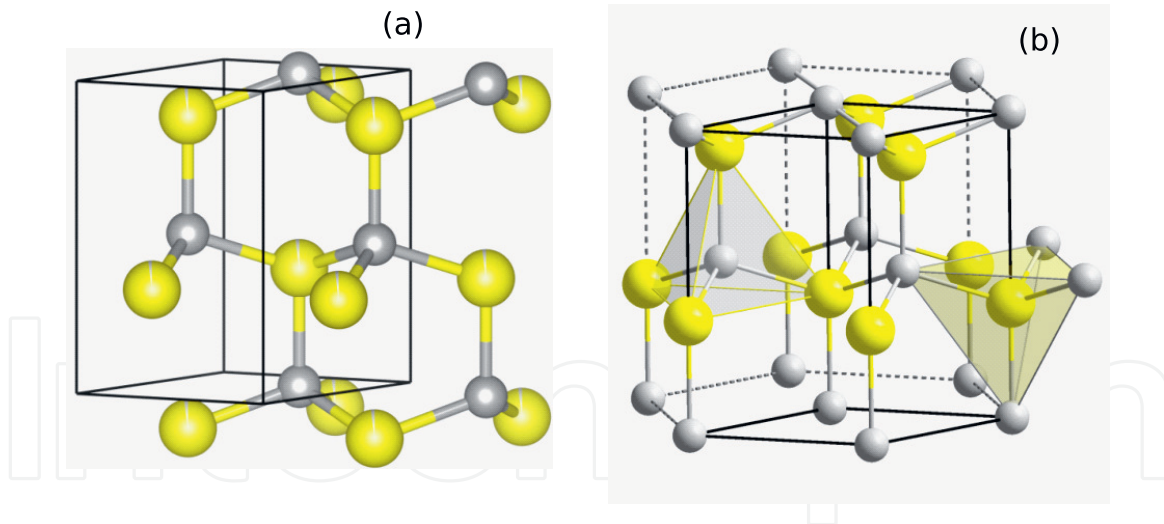


Figure 15.

The non-standard viewing and primitive unit cell of wurtzite ZnO (●-Zn and ●-O). The atomic arrangement is not quite effectively legible and physically meaningful in non-standard viewing, while it is quite meaningful in case of primitive lattice (Table 2).

11. Recommended software packages

1. X-ray diffraction data visualization:

- a. Winplotr [102]
- b. Panalytical X'Pert Highscore
- c. X-Powder
- d. Cyrstal Impact Match [103]
- e. PowderPlot

2. Inter-Conversion of XRD data between different formats

- a. X-powder
- b. PowDLL [104]
- c. Winplotr

3. Search and Match with database

- a. PCPDFWIN from ICDD
- b. Cyrstal Impact Match
- c. X-Powder
- d. Panalytical X'Pert Highscore [105]

4. Indexing

- a. EXPO2014

- b. DICVOL
- c. ITO
- d. TREOR

5. Rietveld Refinement

- a. EdPcr, fp2k from Fullprof suite [102, 106]
- b. Crystal Impact Match
- c. Profex [107]
- d. QualX and Quanto

6. Fourier Map Visualization

- a. GFourier
- b. VESTA [96]

7. Structure Visualization

- a. Crystal Impact Diamond
- b. VESTA

12. Rietveld refinement examples

The case of Rietveld refinement of perovskite LaMnO_3 along with various refinement parameters is given in “Retiveld Refinement ...” section, while two

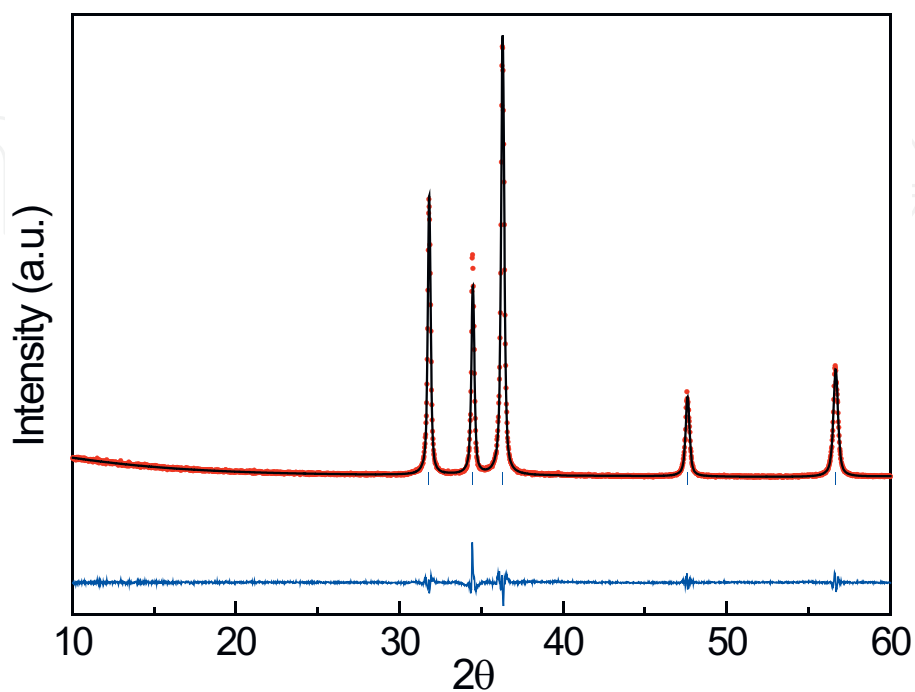


Figure 16.
Representative Rietveld refinement plot of wurtzite ZnO with observed (red circles), calculated (black), difference (blue) and Bragg positions (blue bars).

S. group	χ^2	R_p	R_{wp}	R_{exp}	R_F	R_B	
$P6_3mc$	1.24	8.56	10.9	8.81	1.04	1.2	
Lattice parameters			Fractional coordinates				
a (Å)	c (Å)	Zn			O		
3.254	5.212	x	y	z	x	y	z
		0.3333	0.6667	0.0	0.3333	0.6667	0.3820

Table 2.
Rietveld refined fractional co-ordinates, space group, lattice parameters, R- values (R_p : Un-weighted profile parameter, R_{wp} : Weighted profile parameter, R_{exp} : Expected profile parameter, R_F : Structure parameter, R_B : Intensity parameter), χ^2 : Goodness of fit and other parameters of ZnO.

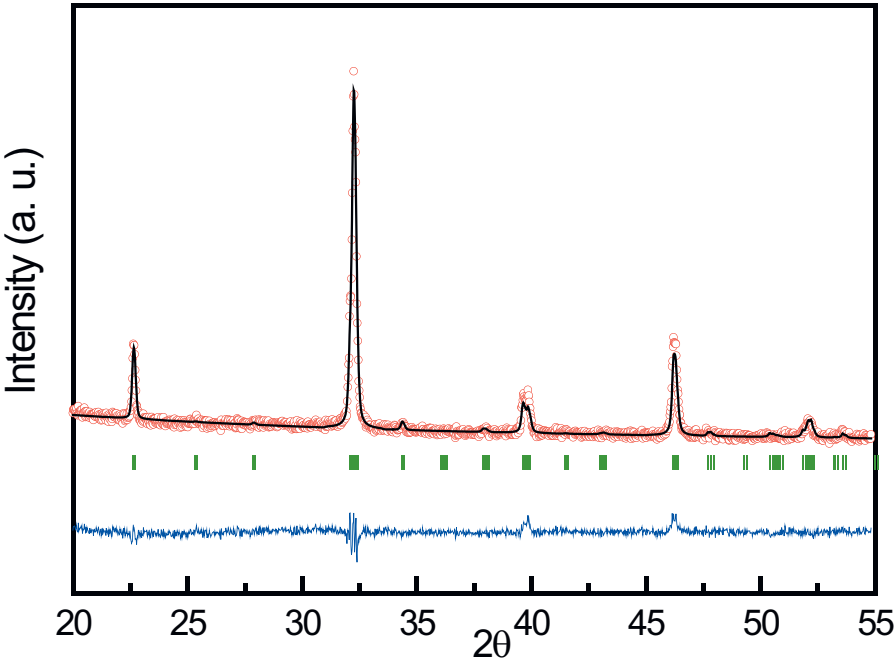


Figure 17.
Representative Rietveld refinement plot of double perovskite La_2FeCoO_6 with observed (red circles), calculated (black), difference (blue) and Bragg positions (green bars).

SG	χ^2	R_p	R_{wp}	R_{exp}	R_F	R_B		
$P\ 21/n$	1.24	4.87	6.34	4.73	5.51	6.05		
Lattice parameters			Fractional coordinates					
a (Å)	b (Å)	c (Å)	La			O		
5.566	5.501	9.666	x	y	z	x	y	z
$\alpha = \gamma = 90^\circ$			0.2434	0.0226	0.2486	0.1793	0.2280	0.9590
						0.23180	0.7221	0.9584
						0.3323	0.0122	0.7555
			Fe			Co		
$\beta = 124.35^\circ$			x	y	z	x	y	z
			0.5	0.0	0.0	0.0	0.0	0.5

Table 3.
Rietveld refined fractional co-ordinates, space group (SG) lattice parameters, R- values (R_p : Un-weighted profile parameter, R_{wp} : Weighted profile parameter, R_{exp} : Expected profile parameter, R_F : Structure parameter, R_B : Intensity parameter), χ^2 : Goodness of fit and other parameters of La_2FeCoO_6 .

additional cases of Wurtzite ZnO and double-perovskite $\text{La}_2\text{FeCoO}_6$ are given here (Figures 16 and 17, Tables 2 and 3):

- a. ZnO
- b. $\text{La}_2\text{FeCoO}_6$

Acknowledgements


The chapter will remain incomplete without the mention of Dr. Vilas Shelke and the hour-long discussions regarding crystal structure and x-ray diffraction which sparked the interest and provided the motivation for detailed studies necessary for the completion of this work. Without availing the facilities and the healthy discussions with Dr. Mukhul Gupta, Dr. V Ganeshan, and Dr. D M Phase from UGC DAE CSR Indore and Prof. S P Sanyal from Barkatullah University Bhopal the work would have remained incomplete.

Author details

Touseef Ahmad Para* and Shaibal Kanti Sarkar
Devices and Interfaces Lab, Department of Energy Science and Engineering, Indian Institute of Technology Bombay, Mumbai, Maharashtra, India

*Address all correspondence to: drtouseefpara@yahoo.com

IntechOpen

© 2021 The Author(s). Licensee IntechOpen. This chapter is distributed under the terms of the Creative Commons Attribution License (<http://creativecommons.org/licenses/by/3.0>), which permits unrestricted use, distribution, and reproduction in any medium, provided the original work is properly cited. 

References

- [1] Glazer AM. The first paper by W.L. Bragg-what and when? *Crystallogr Rev.* 2013;19(3):117–124. DOI: 10.1080/0889311X.2013.813494
- [2] Wilkins SW. Celebrating 100 years of X-ray crystallography. *Acta Crystallogr Sect A Found Crystallogr [Internet]*. 2013;69(1):1–4. DOI: 10.1107/S0108767312048490
- [3] Glazer AM. Celebrating the braggs—A personal account. *Interdiscip Sci Rev.* 2015;40(3):329–39. DOI: 10.1179/0308018815Z.000000000121
- [4] Bragg WH, Bragg WL. The reflection of X-rays by crystals. *Proc R Soc London Ser A, Contain Pap a Math Phys Character [Internet]*. 1913 Jul;88(605):428–38. DOI: 10.1098/rspa.1913.0040
- [5] Glazer AM. The Braggs. *Ferroelectrics.* 2002;267(1):35–41. DOI: 10.1080/00150190211007
- [6] Liljas A. Background to the Nobel Prize to the Braggs. *Acta Crystallogr Sect A Found Crystallogr [Internet]*. 2012/12/20. 2013;69(1):10–5. DOI: 10.1107/S0108767312031133
- [7] Thomson P. A tribute to W. L. Bragg by his younger daughter. *Acta Crystallogr Sect A Found Crystallogr [Internet]*. 2012/12/20. 2013;69(1):5–7. DOI: 10.1107/s0108767312047514
- [8] BRAGG WL. A New Type of ‘X-Ray Microscope.’ *Nature [Internet]*. 1939 Apr;143(3625):678–678. DOI: 10.1038/143678a0
- [9] Perutz MF. How W. L. Bragg invented X-ray analysis. *Acta Crystallogr Sect A [Internet]*. 1990;46(8):633–43. DOI: 10.1107/S010876739000410X
- [10] Bragg WL. The structure of some crystals as indicated by their diffraction of X-rays. *Proc R Soc London Ser A, Contain Pap a Math Phys Character.* 1913;89(610):248–77. DOI: 10.1098/rspa.1913.0083
- [11] Ewald PP. Max von Laue, 1879–1960. *Acta Crystallogr [Internet]*. 1960 Jul 10;13(7):513–5. DOI: 10.1107/S0365110X6000128X
- [12] Laue M Von. Concerning the detection of X-ray interferences [Internet]. Nobel lecture. 1915.
- [13] Scherrer P. Bestimmung der inneren Struktur und der Größe von Kolloidteilchen mittels Röntgenstrahlen. In: *Kolloidchemie Ein Lehrbuch [Internet]*. Berlin, Heidelberg: Springer Berlin Heidelberg; 1912. p. 387–409. DOI: 10.1007/978-3-662-33915-2_7
- [14] Holzwarth U, Gibson N. The Scherrer equation versus the “Debye-Scherrer equation.” *Nat Nanotechnol.* 2011;6(9):534. DOI: 10.1038/nnano.2011.145
- [15] Patterson AL. The scherrer formula for X-ray particle size determination. *Phys Rev.* 1939;56(10):978–82. DOI: 10.1103/PhysRev.56.978
- [16] Visser JW. Modern powder diffraction. Vol. 72, *Sedimentary Geology*. Walter de Gruyter GmbH & Co KG; 1991. 168–170 p. DOI: 10.1016/0037-0738(91)90134-y
- [17] Chernyshev V V. Structure determination from powder diffraction. *Russ Chem Bull [Internet]*. 2001;50(12):2273–92. DOI: 10.1023/A:1015006807065
- [18] Stephens PW, Bendele GM. X-Ray Powder Diffraction. In: *Characterization of Materials [Internet]*. Hoboken, NJ, USA: John Wiley & Sons, Inc.; 2002. DOI: 10.1002/0471266965.com071

- [19] David WIF. Powder diffraction: Least-squares and beyond. *J Res Natl Inst Stand Technol* [Internet]. 2004/01/01. 2004 Jan;109(1):107. DOI: 10.6028/jres.109.008
- [20] Bail A Le. Chapter 5. The Profile of a Bragg Reflection for Extracting Intensities. In: *Powder Diffraction* [Internet]. Cambridge: Royal Society of Chemistry; 2008. p. 134–65. DOI: 10.1039/9781847558237-00134
- [21] Altomare A, Giacovazzo C, Moliterni A. *Powder Diffraction*. Powder Diffraction. 2008. DOI: 10.1039/9781847558237
- [22] Dinnebier RE, Leineweber A, Evans JSO. Rietveld Refinement: Practical Powder Diffraction Pattern Analysis using TOPAS [Internet]. Vol. 52, *Journal of Applied Crystallography*. De Gruyter; 2019. 1238–1239 p. DOI: 10.1515/9783110461381
- [23] Le Bail A, Duroy H, Fourquet JL. Ab-initio structure determination of LiSbWO_6 by X-ray powder diffraction. *Mater Res Bull* [Internet]. 1988;23(3):447–52. DOI: 10.1016/0025-5408(88)90019-0
- [24] Antoniadis A, Berruyer J, Filhol A. Maximum-likelihood methods in powder diffraction refinements. *Acta Crystallogr Sect A* [Internet]. 1990;46(8):692–711. DOI: 10.1107/S0108767390004500
- [25] Hendrickson WA. Evolution of diffraction methods for solving crystal structures. *Acta Crystallogr Sect A Found Crystallogr* [Internet]. 2012/12/20. 2013;69(1):51–9. DOI: 10.1107/S0108767312050453
- [26] Rietveld HM. Line profiles of neutron powder-diffraction peaks for structure refinement. *Acta Crystallogr*. 1967;22(1):151–2. DOI: 10.1107/s0365110x67000234
- [27] Rietveld HM. A profile refinement method for nuclear and magnetic structures. *J Appl Crystallogr*. 1969;2(2):65–71. DOI: 10.1107/s0021889869006558
- [28] Rietveld H. The Rietveld Method ? A Historical Perspective. *Aust J Phys* [Internet]. 1988;41(2):113. DOI: 10.1071/PH880113
- [29] Sakata M, Cooper MJ. An analysis of the Rietveld refinement method. *J Appl Crystallogr* [Internet]. 1979 Dec 1;12(6):554–63. DOI: 10.1107/S002188987901325X
- [30] Hester JR. Improved asymmetric peak parameter refinement. *J Appl Crystallogr* [Internet]. 2013;46(4):1219–20. DOI: 10.1107/S0021889813016233
- [31] Finger LW, Cox DE, Jephcoat AP. Correction for powder diffraction peak asymmetry due to axial divergence. *J Appl Crystallogr* [Internet]. 1994;27(pt 6):892–900. DOI: 10.1107/S0021889894004218
- [32] Dollase WA. Correction of intensities for preferred orientation in powder diffractometry: application of the March model. *J Appl Crystallogr* [Internet]. 1986 Aug 1;19(4):267–72. DOI: 10.1107/S0021889886089458
- [33] Altomare A, Burla MC, Cascarano G, Giacovazzo C, Guagliardi A, Moliterni AGG, et al. Early Finding of Preferred Orientation: Applications to Direct Methods. *J Appl Crystallogr* [Internet]. 1996;29 PART 4(4):341–5. DOI: 10.1107/s0021889896000271
- [34] Para TA, Shelke V. Extreme blue-shifted photoluminescence from quantum confinement of core-shell ZnO . *J Mater Sci Mater Electron* [Internet]. 2017 Dec 1;28(24):18842–8. DOI: 10.1007/s10854-017-7835-0
- [35] Balzar D, Popa NC. Analyzing microstructure by rietveld refinement *. *J Rigaku*. 2005;22(1):16–25.

- [36] Audebrand N, Auffrédic JP, Louër D. An X-ray powder diffraction study of the microstructure and growth kinetics of nanoscale crystallites obtained from hydrated cerium oxides. *Chem Mater*. 2000;12(6):1791–9. DOI: 10.1021/cm001013e
- [37] Von Dreele RB. Multipattern Rietveld refinement of protein powder data: An approach to higher resolution. *J Appl Crystallogr* [Internet]. 2007;40(1):133–43. DOI: 10.1107/S0021889806045493
- [38] Hill RJ, Cranswick LMD. International Union of Crystallography. Commission on Powder Diffraction. Rietveld refinement round robin. II. Analysis of monoclinic ZrO_2 . *J Appl Crystallogr* [Internet]. 1994 Oct;27(5):802–44. DOI: 10.1107/S0021889894000646
- [39] Altomare A, Carrozzini B, Giacovazzo C, Guagliardi A, Moliterni AGG, Rizzi R. Solving Crystal Structures from Powder Data. I. The Role of the Prior Information in the Two-Stage Method. *J Appl Crystallogr* [Internet]. 1996;29 PART 6(6):667–73. DOI: 10.1107/s0021889896007467
- [40] Madsen IC, Scarlett NVY, Cranswick LMD, Lwin T. Outcomes of the International Union of Crystallography Commission on Powder Diffraction Round Robin on Quantitative Phase Analysis: samples 1 a to 1 h. *J Appl Crystallogr* [Internet]. 2001 Aug 1;34(4):409–26. DOI: 10.1107/S0021889801007476
- [41] Hill RJ. International union of crystallography commission on powder diffraction rietveld refinement round Robin. I. Analysis of standard x-ray and neutron data for PbSO_4 . *J Appl Crystallogr*. 1992;25(pt 5):589–610. DOI: 10.1107/S0021889892003649
- [42] Mccusker LB, Von Dreele RB, Cox DE, Louër D, Scardi P. Rietveld refinement guidelines. *J Appl Crystallogr* [Internet]. 1999;32(1):36–50. DOI: 10.1107/S0021889898009856
- [43] Buhrke VE, Jenkins R, Smith DK, Kingsley D. Practical guide for the preparation of specimens for x-ray fluorescence and x-ray diffraction analysis. Wiley-VCH; 1998.
- [44] Bish DL, Reynolds RC. SAMPLE PREPARATION FOR X-RAY DIFFRACTION. In: Bish DL, Post JE, editors. *Modern Powder Diffraction* [Internet]. Berlin, Boston: De Gruyter; 1989. p. 73–100. DOI: 10.1515/9781501509018-007
- [45] Ewald PP. X-ray diffraction by finite and imperfect crystal lattices. *Proc Phys Soc*. 1940;52(1):167–74. DOI: 10.1088/0959-5309/52/1/323
- [46] Hill RJ, Madsen IC. Data Collection Strategies for Constant Wavelength Rietveld Analysis. *Powder Diffr*. 1987;2(3):146–62. DOI: 10.1017/S088571560001263X
- [47] Von Dreele RB, Rodriguez-Carvajal J. Chapter 3. The Intensity of a Bragg Reflection. In: *Powder Diffraction* [Internet]. Cambridge: Royal Society of Chemistry; 2008. p. 58–88. DOI: 10.1039/9781847558237-00058
- [48] Cooper MJ. The analysis of powder diffraction data. *Acta Crystallogr Sect A* [Internet]. 1982 Mar 1;38(2):264–9. DOI: 10.1107/S0567739482000564
- [49] Young RA. The rietveld method. Vol. 6. Oxford university press Oxford; 1993.
- [50] Mccusker LB, Von Dreele RB, Cox DE, Louër D, Scardi P. Rietveld refinement guidelines. *J Appl Crystallogr*. 1999;32(1):36–50. DOI: 10.1107/S0021889898009856
- [51] David WIF, Sivia DS. Background estimation using a robust Bayesian

- analysis. *J Appl Crystallogr* [Internet]. 2001 Jun 1;34(3):318–24. DOI: 10.1107/S0021889801004332
- [52] Langford JI. Accuracy in powder diffraction. In: *Natl Bur Stand Spec Publ. National Bureau of Standards, Gaithersburg, Maryland: US Dept. of Commerce, National Bureau of Standards: for sale by the Supt. of ...*; 1980. p. 255–69.
- [53] Langford JI, Louër D, Scardi P. Effect of a crystallite size distribution on X-ray diffraction line profiles and whole-powder-pattern fitting. *J Appl Crystallogr*. 2000;33(3 II):964–74. DOI: 10.1107/S002188980000460X
- [54] Langford JI, Delhez R, de Keijser TH, Mittemeijer EJ. Profile analysis for microcrystalline properties by the Fourier and other methods. *Aust J Phys*. 1988;41(2):173–87. DOI: 10.1071/PH880173
- [55] Langford JI. Some applications of pattern fitting to powder diffraction data. *Prog Cryst Growth Charact*. 1987;14(C):185–211. DOI: 10.1016/0146-3535(87)90018-9
- [56] Hepp A, Baerlocher C. Learned peak shape functions for powder diffraction data. *Aust J Phys*. 1988;41(2):229–36. DOI: 10.1071/PH880229
- [57] Balzar D. Voigt-function model in diffraction line-broadening analysis. *Int Union Crystallogr Monogr Crystallogr* [Internet]. 1999;10:44.
- [58] Prevey PS. The Use of Person VII Distribution Functions in X-Ray Diffraction Residual Stress Measurement. *Adv X-ray Anal* [Internet]. 1985 Mar 6;29:103–11. DOI: 10.1154/S037603080001017X
- [59] Balzar D. Profile fitting of x-ray diffraction lines and fourier analysis of broadening. *J Appl Crystallogr* [Internet]. 1992;25(pt 5):559–70. DOI: 10.1107/S0021889892004084
- [60] Howard SA, Preston KD. 8. Profile Fitting of Powder Diffraction Patterns. *Mod Powder Diffr*. 2018;20:217–76. DOI: 10.1515/9781501509018-011
- [61] Langford JI. A rapid method for analysing the breadths of diffraction and spectral lines using the Voigt function. *J Appl Crystallogr* [Internet]. 1978 Feb 1;11(1):10–4. DOI: 10.1107/S0021889878012601
- [62] Le Bail A. Monte Carlo indexing with McMaille. *Powder Diffr*. 2004;19(3):249–54. DOI: 10.1154/1.1763152
- [63] Le Bail A, Louër D. Smoothing and validity of crystallite-size distributions from X-ray line-profile analysis. *J Appl Crystallogr* [Internet]. 1978;11(1):50–5. DOI: 10.1107/s0021889878012662
- [64] Le Bail A. The Rietveld method using an experimental profile convoluted by adjustable analytical function. *Acta Crystallogr Sect A Found Crystallogr* [Internet]. 1984;40(a1):C369–C369. DOI: 10.1107/s0108767384089200
- [65] Cranswick LMD, Le Bail A. Beyond classical Rietveld analysis using Le Bail fitting. *Acta Crystallogr Sect A Found Crystallogr* [Internet]. 2002 Aug 6;58(s1):c242–c242. DOI: 10.1107/S0108767302094709
- [66] Pawley GS. Unit-cell refinement from powder diffraction scans. *J Appl Crystallogr* [Internet]. 1981;14(6):357–61. DOI: 10.1107/s0021889881009618
- [67] Baharie E, Pawley GS. Counting statistics and powder diffraction scan refinements. *J Appl Crystallogr* [Internet]. 1983;16(4):404–6. DOI: 10.1107/s0021889883010699
- [68] Hahn T, Shmueli U, Arthur JCW. *International Tables for*

Crystallography. Vol. 16, Journal of Applied Crystallography. Reidel Dordrecht; 1983. 284–284 p. DOI: 10.1107/s0021889883010444

[69] Prince E, Wilson AJC. International Tables for Crystallography. J Appl Crystallogr [Internet]. 1983 Apr 1;16(2): 284–284. DOI: 10.1107/S0021889883010444

[70] Kopsky V, Litvin DB. International Tables for Crystallography. J Appl Crystallogr [Internet]. 1983 Apr 1;16(2): 284–284. DOI: 10.1107/S0021889883010444

[71] Bryan RF. International Tables for Crystallography. J Appl Crystallogr [Internet]. 1983 Apr 1;16(2):284–284. DOI: 10.1107/S0021889883010444

[72] Cullity BD. Elements of X-ray Diffraction. Addison-Wesley Publishing; 1956.

[73] Von Dreele RB. Quantitative texture analysis by Rietveld refinement. J Appl Crystallogr. 1997;30(4):517–25. DOI: 10.1107/S0021889897005918

[74] Altomare A, Ciriaco F, Cuocci C, Falcicchio A, Fanelli F. Combined powder X-ray diffraction data and quantum-chemical calculations in EXPO2014. Powder Diffr. 2017;32(S1): S123–8. DOI: 10.1017/S088571561700015X

[75] Hill RJ. Expanded Use of the Rietveld Method in Studies of Phase Abundance in Multiphase Mixtures*. Powder Diffr. 1991;6(2):74–7. DOI: 10.1017/S0885715600017036

[76] Bish DL, Chipera SJ. Accuracy in Quantitative X-ray Powder Diffraction Analyses. Adv X-ray Anal. 1994;38:47–57. DOI: 10.1154/s0376030800017638

[77] Parrish W, Huang TC. Accuracy of the Profile Fitting Method for X-Ray Polycrystalline Diffractometry. Vol. 567,

National Bureau of Standards, Special Publication. 1979. 95–110 p.

[78] Cline JP. Accuracy in powder diffraction III - Part 1 - Preface. J Res Natl Inst Stand Technol [Internet]. 2004 Jan;109(1):iii. DOI: 10.6028/jres.109.001

[79] Hill RJ, Flack HD. The use of the Durbin–Watson d statistic in Rietveld analysis. J Appl Crystallogr. 1987;20(5): 356–61. DOI: 10.1107/S0021889887086485

[80] Block S, Hubbard CR. Accuracy in powder diffraction: proceedings of a Symposium on Accuracy in Powder Diffraction held at the National Bureau of Standards, Gaithersburg, Maryland, June, 11–15, 1979 [Internet]. Vol. 567. US Dept. of Commerce, National Bureau of Standards: for sale by the Supt. of~ ... ; 1980.

[81] Newsam JM, Deem MW, Freeman CM. Direct Space Methods of Structure Solution From Powder Diffraction Data. In: Accuracy in powder diffraction II: NIST Special Publication. 1992. p. 80–91.

[82] Woolfson MM. An Introduction to X-ray Crystallography [Internet]. Cambridge University Press; 1997. DOI: 10.1017/CBO9780511622557

[83] Smith F. Industrial Applications of X-Ray Diffraction [Internet]. Smith F, editor. CRC Press; 1999. DOI: 10.1201/b16940

[84] Stanjek H, Häusler W. Basics of X-ray diffraction. Hyperfine Interact [Internet]. 2004;154(1–4):107–19. DOI: 10.1023/B:HYPE.0000032028.60546.38

[85] Toby BH. R factors in Rietveld analysis: How good is good enough? . Powder Diffr. 2006;21(1):67–70. DOI: 10.1154/1.2179804

[86] Post JE, Bish DL. Rietveld refinement of crystal structures using

- powder x-ray diffraction data. In: Bish DL, Post JE, editors. *Modern Powder Diffraction* [Internet]. Berlin, Boston: De Gruyter; 1989. p. 277–308. DOI: 10.1515/9781501509018-012
- [87] Cox DE, Papoular RJ. Structure Refinement with Synchrtron Data: R-Factors, Errors and Significance Tests. *Mater Sci Forum* [Internet]. 1996 Jul; 228–231(PART 1):233–8. DOI: 10.4028/www.scientific.net/MSF.228-231.233
- [88] Berar JF, Lelann P. E.S.D.'s and estimated probable error obtained in rietveld refinements with local correlations. *J Appl Crystallogr*. 1991;24 (pt 1):1–5. DOI: 10.1107/S0021889890008391
- [89] de Keijser T, Mittemeijer EJ, Rozendaal HCF. The determination of crystallite-size and lattice-strain parameters in conjunction with the profile-refinement method for the determination of crystal structures. *J Appl Crystallogr* [Internet]. 1983 Jun 1; 16(3):309–16. DOI: 10.1107/S0021889883010493
- [90] Lutterotti L, Scardi P. Simultaneous structure and size-strain refinement by the rietveld method. *J Appl Crystallogr*. 1990;23(4):246–52. DOI: 10.1107/S0021889890002382
- [91] Caglioti G, Paoletti A, Ricci FP. Choice of collimators for a crystal spectrometer for neutron diffraction. *Nucl Instruments*. 1958;3(4):223–8. DOI: 10.1016/0369-643X(58)90029-X
- [92] Bienenstock A, Ewald PP. Symmetry of Fourier space. *Acta Crystallogr*. 1962;15(12):1253–61. DOI: 10.1107/s0365110x6200331x
- [93] Bindzus N, Iversen BB. Maximum-entropy-method charge densities based on structure-factor extraction with the commonly used Rietveld refinement programs GSAS, FullProf and Jana2006. *Acta Crystallogr Sect A Found* Crystallogr [Internet]. 2012/10/19. 2012; 68(6):750–62. DOI: 10.1107/S0108767312037269
- [94] Bushmarinov IS, Dmitrienko AO, Korlyukov AA, Antipin MY. Rietveld refinement and structure verification using Morse restraints. *J Appl Crystallogr* [Internet]. 2012;45(6):1187–97. DOI: 10.1107/S0021889812044147
- [95] Alcock NW, Pawley GS, Rourke CP, Levine MR. An improvement in the algorithm for absorption correction by the analytical method. *Acta Crystallogr Sect A* [Internet]. 1972;28(5):440–4. DOI: 10.1107/S0567739472001159
- [96] Momma K, Izumi F. VESTA: A three-dimensional visualization system for electronic and structural analysis. *J Appl Crystallogr*. 2008;41(3):653–8. DOI: 10.1107/S0021889808012016
- [97] Glazer AM. The classification of tilted octahedra in perovskites. *Acta Crystallogr Sect B Struct Crystallogr Cryst Chem*. 1972;28(11):3384–92. DOI: 10.1107/s0567740872007976
- [98] Glazer AM. Simple ways of determining perovskite structures. *Acta Crystallogr Sect A*. 1975;31(6):756–62. DOI: 10.1107/S0567739475001635
- [99] Glazer AM, Mabud SA. Powder profile refinement of lead zirconate titanate at several temperatures. II. Pure PbTiO₃. *Acta Crystallogr Sect B Struct Crystallogr Cryst Chem*. 1978;34(4): 1065–70. DOI: 10.1107/s0567740878004938
- [100] Para TA, Reshi HA, Pillai S, Shelke V. Grain size disposed structural, optical and polarization tuning in ZnO. *Appl Phys A* [Internet]. 2016 Aug 12;122 (8):730. DOI: 10.1007/s00339-016-0256-8
- [101] Para TA, Reshi HA, Shelke V. Synthesis of ZnSnO₃ nanostructure by sol gel method. In: AIP Conference

Proceedings [Internet]. 2016.
p. 050002. DOI: 10.1063/1.4947656

[102] Roisnel T, Rodríguez-Carvajal J.
WinPLOTR: A Windows Tool for
Powder Diffraction Pattern Analysis.
Mater Sci Forum [Internet]. 2001 Oct;
378–381(I):118–23. DOI: 10.4028/www.
scientific.net/MSF.378-381.118

[103] Putz H, Brandenburg K G. Match!
– Phase identification from powder
diffraction, crystal impact.
Kreuzherrenstr. 102, 53227 Bonn,
Germany [Internet]. Crystal Impact;
2018. p. 10.

[104] Kourkouvelis N. PowDLL, a
reusable .NET component for
interconverting powder diffraction data:
Recent developments, ICDD Annual
Spring Meetings [Internet]. O'Neill L,
editor. Vol. 28, Powder Diffraction.
2013. p. 137–48. DOI: 10.1017/
S0885715613000390

[105] Degen T, Sadki M, Bron E,
König U, Nénert G. The HighScore
suite. Powder Diffr [Internet]. 2014 Dec
30;29(S2):S13–8. DOI: 10.1017/
S0885715614000840

[106] Rodríguez-Carvajal J. Recent
advances in magnetic structure
determination by neutron powder
diffraction. Phys B Condens Matter
[Internet]. 1993 Oct;192(1–2):55–69.
DOI: 10.1016/0921-4526(93)90108-I

[107] Doebelin N, Kleeberg R. Profex: A
graphical user interface for the Rietveld
refinement program BGMN. J Appl
Crystallogr [Internet]. 2015/10/27. 2015;
48(5):1573–80. DOI: 10.1107/
S1600576715014685